Volume 1 | Number 1 | Jan 2013 | Pages 1–100

RSC Advances

www.rsc.org/advances

ROYAL SOCIETY OF CHEMISTRY

www.rsc.org/advances

RSC Advances

ARTICLE TYPE

Naked-eye-based selective detection of pyrophosphate with Zn²⁺ complex in aqueous solution and electrospun nanofibers

Zhanxian Li,* Wenying Zhang, Xingjiang Liu, Chunxia Liu, Mingming Yu,* Liuhe Wei*

A mononuclear zinc complex is shown to act as a highly selective naked-eye-based chemosensor for pyrophosphate (PPi) in aqueous solution. Based on the keto-enol transformation process, addition of PPi made the color of the sensor complex change from red to colorless. Moreover, electrospun nanofiber from the mononuclear zinc complex could detect PPi on site and real-time and the color of the nanofiber
10 changes rapidly after it was immersed into aqueous solution of pyrophosphate.

Introduction

The development of anion recognition systems has become an important research field. It is very important to selectively detect the anion pyrophosphate $P_2O_7^{4-}$ (PPi) because PPi is the product
15 of ATP hydrolysis under cellular conditions[1] and it is involved in DNA replication catalyzed by DNA polymerase.[2] In addition, its detection has become more and more important in cancer research in the recent years.[3] Up to now, most of the reported chemosensors for PPi are based on fluorescence change and used
20 in solution,[4] and very few examples about colorimetric chemical sensors for PPi were reported.[5] As well known, fluorescent sensors normally depend on emission intensity or position change and could be significantly influenced by excitation power and detector sensitivity. To contrast, color changes based on
25 absorption properties of the ground state are more suitable for direct observation with the naked eye.[6]

Proton transfer plays a critical role in many chemical, photochemical, catalytic, and biomolecular processes and it is a hot topic in today's scientific research.[7] Proton transfer reactions
30 can be classified and identified by the reaction in the ground or excited states.[8] On the basis of the ESIPT mechanism, various fluorescent sensors have been developed because of their unique and outstanding spectral sensitivity to the environmental mediu.[9] For instance, 8-hydroxyquinoline (8-HQ) and its derivatives have
35 been widely used as fluorescent sensors for cellular and environmental metal ions because metal binding to 8-HQ can block the excited-state intramolecular proton transfer (ESIPT) channel and revive fluorescence.[10] In fact, several quinoline-ligated zinc complexes have been developed as fluorescent
40 chemosensors for PPi.[11] However, ground-state tautomerism including ground-state reverse proton transfer (GSRPT) process was mainly investigated by theoretical methods[12] and spectroscopic techniques[13] The phenomenon of enol−keto tautomeric transformation in the ground state has been
45 observed,[14] and no example of sensors based on ground-state intramolecular proton transfer has been reported except our

previous work.[15]

Conventionally, the chemical sensors are applied to detect target chemicals in solution and the color or fluorescence changes
50 result from the reaction with the target. In the same time, the sensor may also interfere with the cell or tissue that releases the chemicals. That is to say, such a sensor is invasive. Compared with the conventional chemical sensors, a solid-state sensor is non-invasive and it transforms the real-time chemical
55 concentration into electronic signals without interference with the biological processes under study, so it is necessary to develop solid-state chemical sensors for biomedical and medicine.[16] On the other hand, Electrospinning is an effective and simple method for preparing various composite nanofibers. It is a process which
60 uses a strong electrostatic force by a high static voltage applied to a polymer solution placed into a container that has a millimetre diameter nozzle. Because nanofibers prepared by electrospinning have large surface area-to-volume ratio, unique nanoscale architecture, and simple and cost-effective preparation method,
65 they have been proved to be excellent host materials for developing functional materials.[17] Nanofibrous film can have approximately 1−2 orders of magnitude more surface area than that found in continuous thin films. It is expected this large amount of available surface area has the potential to provide
70 unusually high sensitivity and fast response time in sensing application.[18] As a result, such electrospun nanofibres are becoming more and more popular as matrices for optical sensors.[19] To date, most of the studies on the PPi-sensors are stressed on the design of selective fluorescent probes dissolved in
75 aqueous or polar organic solvents. In contrast, the investigation of sensors on the solid matrices has been rarely studied.[20]
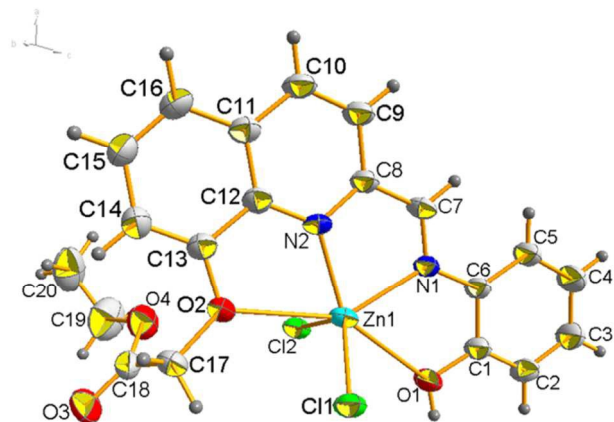
Fig. 1 X-ray crystal structure of complex **ZnLCl₂**.

In our previous work, based on ground-state intramolecular proton transfer, we have prepared three colorimetric sensors for
5 C1−C4 alcohols and studied their photophysical properties. As we have demonstrated, alcohol can mediate ground-state intra-molecular proton transfer, which results in the color change of the sensors. If we use the sensors as the ligand to coordinate zinc ion, can the coordination of the phenolic hydroxyl group to zinc ion
10 inhibit the process of ground-state intra-molecular proton transfer? In this paper, we synthesized a mononuclear zinc complex **ZnLCl₂ (Fig. 1)** employing a derivative of 8-hydroxyquinoline (*E*)-2-(2-Hydroxyphenylimino)-8-(oxygen acetate)-quinoline (**L**) and ZnCl₂. the complex **ZnLCl₂** has good selectivity toward PPi
15 in aqueous solution. Furthermore, we developed a solid-state PPi sensor with electrospinning fibers containing **ZnLCl₂**. The color of the above electrospun nanofibers can also change from red to colorless, indicating its potential application in sensing PPi as a solid-state sensor.

20 ## Results and discussions

Synthesis of the complex ZnLCl₂ and nanofibers

In this work, the complex **ZnLCl₂** was synthesized via the reaction of compound **L** with ZnCl₂, the molecular structure of this complex was confirmed by ^{1}H NMR, and X-ray crystal
25 structure determination. The **ZnLCl₂** molecules are blended with a host polymer, polyvinyl alcohol, and the polymer containing the sensor **ZnLCl₂** was made in fiber form via electrospinning. The morphologies of the nanofibers were confirmed by SEM.
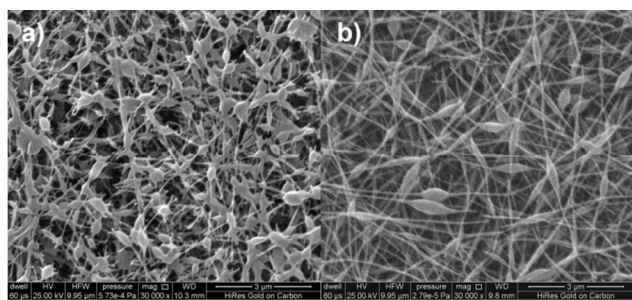
30 **Fig. 2** SEM images of polyvinyl alcohol blending (a) and without (b) **ZnLCl₂** electrospun nanofibers.

Morphologies of electrospinning nanofibers

A typical SEM image of polyvinyl alcohol blending **ZnLCl₂**

nanofibrous film is shown in the left of **Fig. 2**. It can be seen that
35 the film was composed of numerous, randomly oriented nanofibers. In this work, the beads on the fibers were formed during electrospinning of a 10wt% polyvinyl alcohol blending **ZnLCl₂** (2.96 × 10^{-2} wt%) solution. To confirm the appearance reason of the beads, a SEM image of pure polyvinyl alcohol
40 nanofibers has been done (right of **Fig. 2**). As shown in the right of **Fig. 2**, a large number of beads are visible on the PVA nanofibers without ZnLCl₂, implying that such bead defects may not be caused by the dopant ZnLCl₂.

Effect of water and HEPES on the absorption spectroscopy of
45 ZnLCl₂

As we studied in our previous work, the absorption spectrum of compound **L** in ethanol was very sensitive to water.[15] The absorbance peak intensity of sensor **L** (in the previous work, L referred to compound **3**) in the range 400–600 nm decreased
50 quickly upon slow addition of water to its ethanol solution. When the volume ratio of added water to ethanol is about 5%, the color of the ethanol solution changed from red to colorless. As for the complex **ZnLCl₂**, the condition is very different. Upon slow addition of water, the absorption spectroscopy of **ZnLCl₂** (6 ×
55 10^{-5} M) in ethanol changed very little, even when the concentration of water was 3.71 M, the absorbance intensity at 514 nm only changed from 0.27 to 0.207 (left of **Fig. 3**). Such difference between the absorption spectral change of compound **L** and its corresponding complex **ZnLCl₂** indicates that the
60 coordination of ZnCl₂ to **L** inhibits the keto-enol transformation process in the presence of water. In addition, the effect experiment of HEPES on the absorption spectroscopy of **ZnLCl₂** was also done (right of **Fig. 3**). It can be seen that addition of trace HEPES (pH 7.4) can increase the absorbance intensity at
65 504 nm of **ZnLCl₂**, which can be ascribed to the weak basicity. Considering the wide application of HEPES, a mixture of ethanol and HEPES [ethanol/HEPES (pH 7.4) = 10, v/v] was selected as our detection system.
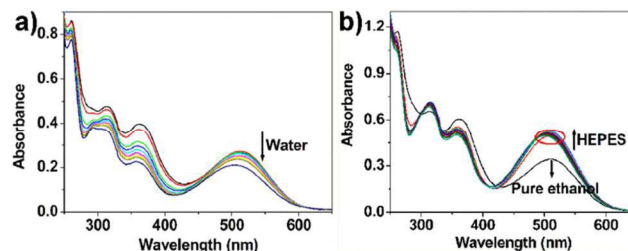
70 **Fig. 3** Absorption spectroscopy change of **ZnLCl₂** (6 × 10^{-5} M) in ethanol upon addition of water (the concentration of water changes from 0 to 3.71 M.) (a) and HEPES (the concentration of HEPES changes from 0 to 3.71 M.) (b).

Effect of PPi on the absorption spectra of ZnLCl₂ and the
75 study of the recyclability of the chemosensor to PPi

Addition of 1.5 equiv. of Na₄P₂O₇ (PPi, 2.5 × 10^{-5} M), into the aqueous solution of **ZnLCl₂** (ethanol/water = 10, v/v) produced a decrease of the absorbance peak intensity at 504 nm and the color changed from red to colorless (**Fig. 4**), implying that complex
80 **ZnLCl₂** can detect PPi by colorimetric method and PPi can be detected with naked-eye with **ZnLCl₂**. Such absorption spectra change may be ascribed to the following reason: PPi has stronger coordination ability than the oxygen of the phenolic hydroxyl

group, so when PPi was introduced to the aqueous solution of **ZnLCl₂**, PPi coordinate zinc ion and the oxygen of the phenolic hydroxyl group was released, which process resulted in the formation of compound **L** and thus brought about the
5 occurrence of the keto–enol transformation in the presence of trace water (**Scheme 1**).[7, 11] **Fig. 5** indicates the absorbance intensity of **ZnLCl₂** (6.0×10^{-5} M) in aqueous solution [ethanol/HEPES (7.4) = 10, v/v] as a function of PPi concentration. In the concentration range of 1.2×10^{-5} M and 9.0
10 $\times 10^{-5}$ M, the absorption peak of **ZnLCl₂** is in good linear relationship with PPi concentration, implying that PPi can be quantitatively detected in a wider concentration range. The binding constant of **L** with Zn^{2+} under identical condition was measured as $1.1 \times 10^{6} M^{-1}$ (**Fig. S1** in Supporting Information),
15 which is much smaller than that of PPi with Zn^{2+}.[21]
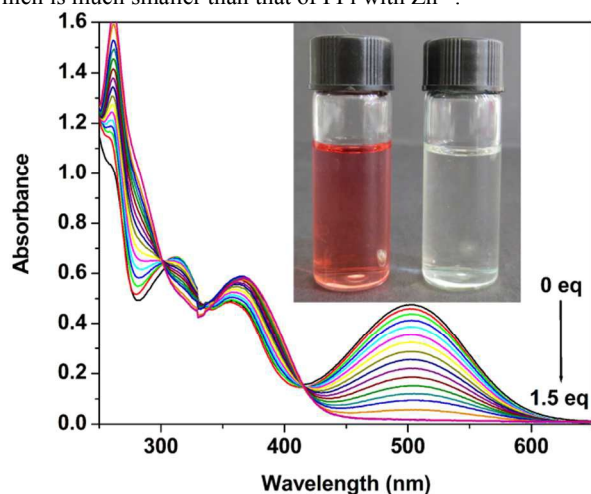
Fig. 4 Absorption spectral change of sensor **ZnLCl₂** (6.0×10^{-5} M) in aqueous solution [ethanol/HEPES (pH 7.4) = 10, v/v] upon addition of Na₄P₂O₇. Inset: Photographs of sensor **ZnLCl₂** (6.0×10^{-5} M) in aqueous
20 solution [ethanol/HEPES (pH 7.4) = 10, v/v] before (left) and after (right) addition of 1.5 equiv. of Na₄P₂O₇.
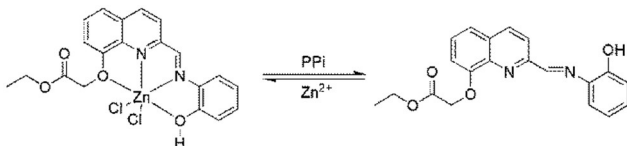
Scheme 1 Proposed recognition mechanism of **ZnLCl₂** toward PPi.

The PPi sensing mechanism was studied by ^1H NMR, ^{13}C
25 NMR and Mass spectra of the isolated product from the reaction of **ZnLCl₂** and PPi (Figures **S2** and **S3** in Supporting Information). The ^1H NMR, ^{13}C NMR, and Mass spectra analysis corroborated that compound **L** was obtained in the reaction of **ZnLCl₂** with PPi.[22] In addition, The single crystals of the isolated product
30 product suitable for X-ray diffraction were grown by slow evaporation of the ethanol solution for several days. The X-ray crystal structure of the isolated product (compound **L**) was shown in **Fig. 6** and the X-ray crystal data was selected.[23]

To examine the recyclability of the chemosensor to PPi, a
35 water solution of ZnCl₂ (2.5×10^{-2} M) was added to the **ZnLCl₂−PPi** solution. When ZnCl₂ was added to the **ZnLCl₂−PPi** solution absorption spectral signals identical to those of **ZnLCl₂** were restored (**Fig. 7**), demonstrating that the

free compound **L** which has originated from the reaction of
40 **ZnLCl₂** and PPi reacted again with ZnCl₂ and reformed the chemosensor **ZnLCl₂**. such experimental result also proved our proposed sensing mechanism.
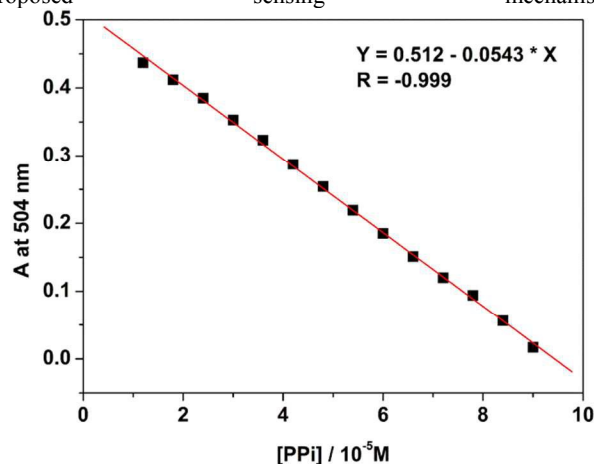
Fig. 5 Plot of absorbance intensity of **ZnLCl₂** (6.0×10^{-5} M) in aqueous
45 solution [ethanol/HEPES (pH 7.4) = 10, v/v] as a function of PPi concentration. A represents the absorbance intensity at 504 nm.
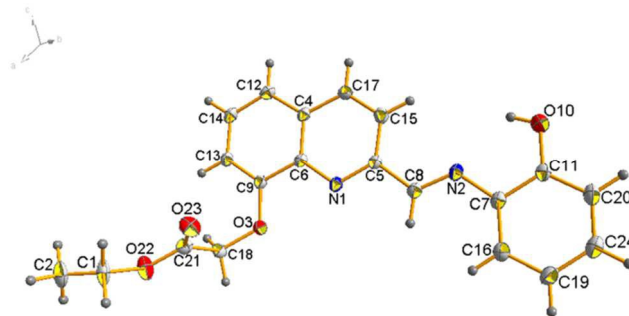
Fig. 6 X-ray crystal structure of the isolated product from the reaction of **ZnLCl₂** with PPi.

50
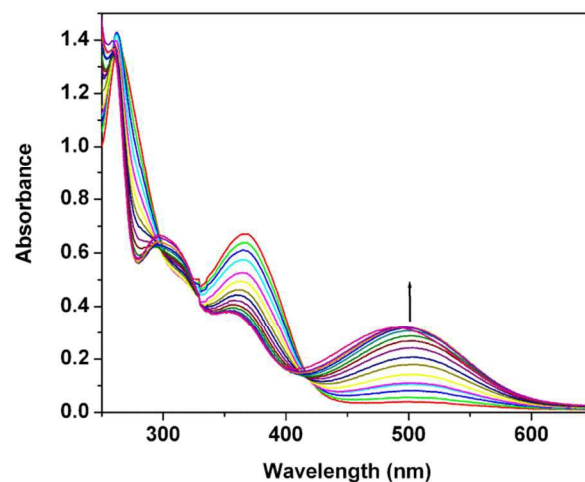
Fig. 7 Absorption spectra change of **ZnLCl₂-PPi** [ethanol/HEPES (pH 7.4) = 10, v/v] solution upon addition of ZnCl₂ water solution (the concentration were 0, 2.4×10^{-5} M, 4.8×10^{-5} M, 7.2×10^{-5} M, 1.2×10^{-4} M, 1.8×10^{-4} M, and 2.4×10^{-4} M.).

55 **The specificity of ZnLCl₂ toward PPi and the competition experiments for ZnLCl₂**

As shown in **Fig. 8** and red bars of **Fig. 9** upon addition of the same amount of the various anions (9.0×10^{-5} M), respectively, only PPi decreased the absorbance intensity of **ZnLCl$_2$** (A/A$_0$ = 0.025, A and A$_0$ represent the absorbance intensity at 504 nm) and changed the color of the solution from red to colorless. However, under identical conditions, nearly no absorbance intensity changes were observed in absorption spectra with NaF, NaCl 、 NaBr, NaI, Na$_2$CO$_3$, NaCH$_3$COO, NaNO$_3$, NaSCN, NaHCO$_3$, Na$_2$SO$_4$, NaNO$_2$, Na$_2$SO$_3$, NaHSO$_3$, NaClO$_4$, NaN$_3$, Na$_2$SiO$_2$, and NaClO$_3$. That is, sensor **ZnLCl$_2$** can readily distinguish PPi from environmentally and biologically relevant anions by absorption spectra. The competition experiments were also conducted for **ZnLCl$_2$** (green bars in **Fig. 9**).When 1.5 equiv. of PPi was added into the solution of **ZnLCl$_2$** in the presence of 1.5 equiv. of anions, similar absorption spectra change was displayed to that with PPi ion only. Such experiments demonstrate that other anions have no influence on the detection of PPi with **ZnLCl$_2$**.

Effect of pH on the recognition process

The pH value of solution was found to be essential to the recognition process. To investigate the pH effect, the absorbance intensities of 60 μM chemosensor **ZnLCl$_2$** at 504 nm in the absence and presence of 90 μM PPi were examined at pH range from 1.0 to 14.0. As shown in **Fig. S4** in Supporting Information, the chemosensor **ZnLCl$_2$** itself shows constant absorbance at 504 nm from pH 7.0 to 8.0, and great decrease in the absorbance at 504 nm was obtained whether in the range from 1 to 7 or 8 to 14. Such great influence on the absorbance intensity at 504 nm of **ZnLCl$_2$** may be ascribed to the effect of pH on the coordination ability of **L** with Zn^{2+}. Upon the addition of PPi, there was no absorbance at 504 nm in pH range of 1.0–14, indicating that compound L has no absorbance at 504 nm in such condition.
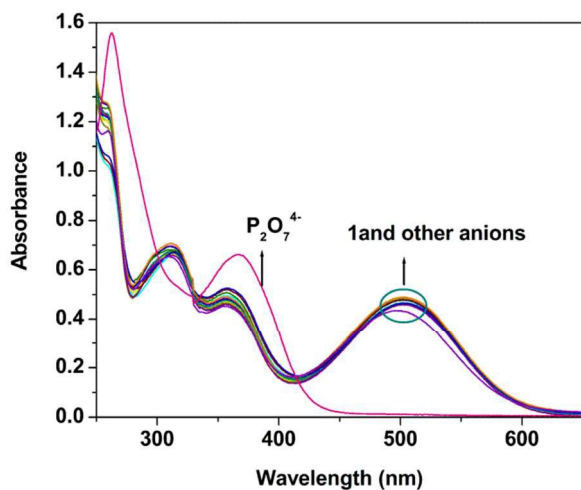
Fig. 8 UV-vis spectra changes of **ZnLCl$_2$** (6.0×10^{-5} M) in aqueous solution [ethanol/HEPES (pH 7.4) = 10, v/v] upon addition of different anions (Na$_4$P$_2$O$_7$, NaF, NaCl, NaBr, NaI, Na$_2$CO$_3$, NaCH$_3$COO, NaNO$_3$, NaSCN, NaHCO$_3$, Na$_2$SO$_4$, NaNO$_2$, Na$_2$SO$_3$, NaHSO$_3$, NaClO$_4$, NaN$_3$, Na$_2$SiO$_2$ and NaClO$_3$, 9.0×10^{-5} M).
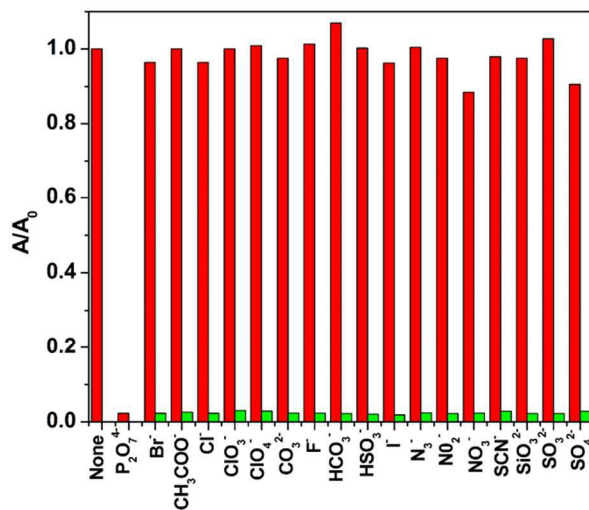
Fig. 9 Absorption spectral responses of **ZnLCl$_2$** [6.0×10^{-5} M, ethanol/HEPES (pH 7.4) = 10, v/v] upon addition of different sodium salts (the ratio of salt ion to **ZnLCl$_2$** is 1.5 equiv., red bars) and absorption spectral change of the mixture of **ZnLCl$_2$** and PPi after addition of the same amount of the appropriate anions (green bars). A and A$_0$ represent the absorbance intensity at 504 nm. The anion salts represent Na$_4$P$_2$O$_7$, NaF, NaCl, NaBr, NaI, Na$_2$CO$_3$, NaCH$_3$COO, NaNO$_3$, NaSCN, NaHCO$_3$, NaSO$_4$, NaNO$_2$, NaSO$_3$, NaHSO$_3$, NaClO$_4$, NaN$_3$, Na$_2$SiO$_2$ and NaClO$_3$.

Response of electrospinning test strip toward different anions

The colorimetric behavior of the electrospinning test strip was investigated in aqueous solution (ethanol/water = 1, v/v) (**Fig. 10**). The test strips were immersed into aqueous solutions (ethanol/water = 1, v/v) of different anions respectively to examine the selectivity of the test strips. As expected, the film showed red color in aqueous solution. Upon addition of different anions, only PPi can induce remarkable color change from red to colorless (**Fig. 1b**). Other representative anions, such as F$^-$, Cl$^-$, Br$^-$, I$^-$, CO$_3^{2-}$, CH$_3$COO$^-$, NO$_3^-$, SCN$^-$, HCO$_3^-$, SO$_4^{2-}$, NO$_2^-$, SO$_3^{2-}$, HSO$_3^-$, ClO$_4^-$, N$_3^-$, SiO$_2^{2-}$, and ClO$_3^-$ showed almost negligible effects on the color behavior of the test strips.

Fig. 10 Photographs of sensor **ZnLCl$_2$** (6.0×10^{-5} M) in aqueous solution [ethanol/HEPES (pH 7.4) = 10, v/v] (**a**) and as electrospinning test strip; (**b**) before (left) and after addition of 1.5 equiv. of different sodium salts (from left to right: blank, Na$_4$P$_2$O$_7$, NaF, NaCl, NaBr, NaI, Na$_2$CO$_3$, NaCH$_3$COO, NaNO$_3$, NaSCN, NaHCO$_3$, NaSO$_4$, NaNO$_2$, NaSO$_3$, NaHSO$_3$, NaClO$_4$, NaN$_3$, Na$_2$SiO$_2$ and NaClO$_3$).

Experimental section

Instruments

^{1}H NMR spectra were recorded on a Bruker 400 NMR spectrometer. Chemical shifts are reported in parts per million using tetramethylsilane (TMS) as the internal standard.

Single-crystal data of the zinc complex was collected on a Bruker SMART APEX CCD diffractometer with graphite-monochromated MoKα radiation (λ = 0.71073 Å) using the ω-

scan technique at room temperature.[24] Empirical absorption corrections were applied to the intensities using the SADABS program.[25] The structure was solved using the program SHELXS-97[26] and refined with the program SHELXL-97.[27] All non-hydrogen atoms were refined anisotropically on F2 by the full-matrix least-squares technique. The hydrogen atoms of the organic ligands were included in the structure factor calculation at idealized positions using a riding model and refined isotropically.

All spectral characterizations were carried out in HPLC-grade solvents at 20 °C within a 10 mm quartz cell. UV–vis absorption spectra were measured with a TU-1901 double-beam UV–vis spectrophotometer. The morphologies of the final products were examined using a FEI Quanta 200 scanning electron microscope (SEM), with an acceleration voltage of 25 kV.

Materials and reagents

All commercial grade chemicals and solvents were purchased and were used without further purification. The (*E*)-2-(2-hydroxyphenylimino)-8-(oxygen acetate)-quinoline (**L**) was synthesized by following our recently reported method (**Scheme 2**).[15]
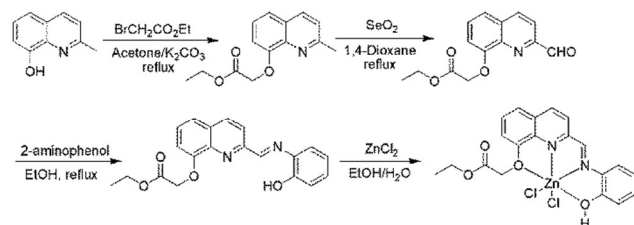
Scheme 2 Synthetic route of **ZnLCl$_2$**.

Synthesis of ZnLCl$_2$

8-(Oxygen acetate)-quinoline-2-aldehyde (173.5 mg, 6.70×10^{-4} mol) and 2-aminophenol (73.1 mg, 6.70×10^{-4} mol) were mixed in 10 mL ethanol and the mixture was refluxed for 2 h under nitrogen atmosphere. After the solvent was removed under reduced pressure, the product was recrystallized from ethanol (199.3 mg, 85%).

Characterization of **L**: Mp = 159−160 °C. HRMS (EI) m/z: calcd for $C_{20}H_{18}N_2O_4$ [M + Na]$^+$, 373.1159; found, 373.1169. ^{1}H NMR (400 MHz, CDCl$_3$, TMS): δ_H 9.14(s, 1H), 8.38 (m, 1H), 8.25 (m, 1H), 7.50 (m, 1H), 7.42 (s, 1H), 7.26 (m, 2H), 7.04 (m, 2H), 6.96 (m, 2H), 5.02 (s, 2H), 4.31 (q, 2H), and 1.30 (t, 3H). ^{13}C NMR (100 MHz, CDCl$_3$): δ_C 168.63, 157.50, 153.89, 153.61, 152.91, 139.96, 136.70, 134.36, 130.27, 127.93, 120.97, 120.40, 118.96, 116.40, 115.39, 110.25, 66.37, 61.57, and 14.22.

A 0.5 mL water solution of ZnCl$_2$ (6.8 mg, 0.05 mmol) was added slowly into a 10 mL ethanol solution of **L** (17.5 mg, 0.05 mmol), and the mixture was stirred for 10 min. And then the mixture was filtered and the filtrate was transferred into a test tube. The single crystals of **ZnLCl$_2$** suitable for X-ray diffraction were grown by slow evaporation of the above filtrate for several days. Yield: 17.4 g, 72%.

The crystal structure was shown in **Fig. 1**, the relevant crystal data and structural parameters are: formula: $C_{20}H_{18}Cl_2N_2O_4Zn$. M = 486.63, triclinic. Unit cell parameters: a = 9.6068(10) Å, b = 9.8747(15) Å, c = 11.0893(14) Å. α = 95.233(12)°, β = 102.357(10)°, γ = 90.567(11)°, V = 1022.9(2) Å^3, T = 291(2) K,

space group P-1, Z = 2, 7862 reflections collected, 3878 independent reflections [R(int) = 0.0536]. Final R indices [I > 2σ(I)] R1 = 0.0716 and wR2 = 0.0951. R indices (all data) R1 = 0.1889 and 0.2209.

Characterization of **ZnLCl$_2$**: TOF MS m/z: calcd for $C_{20}H_{17}Cl_2N_2O_4Zn$ [M - 2], 484; found, 484. ^{1}H NMR (400 MHz, DMSO, TMS): δ_H 9.33 (s, 1H), 8.93 (S, 1H), 8.56 (m, 1H), 8.45 (m, 1H), 7.62 (m, 2H), 7.44 (m, 1H), 7.18 (m, 2H), 6.97 (m, 1H), 6.88 (m, 1H), 5.13 (s, 2H), 4.20 (q, 2H), 1.23 (t, 3H).

Preparation of electrostatic spinning solution and film

The mixture of 26 g deionized water and 3.0000 g polyvinyl alcohol was stirred for 2 h at 80 °C. The DMSO solution (the weight of DMSO was 1.0000 g) of 0.0088 g crystals **ZnLCl$_2$** was slowly added to the above mixture when its temperature was cooled to room temperature, and stirred for about 30 min. Thus the resulting clear homogenous solution with polyvinyl alcohol concentration of 10 % was used for electrospinning the film.

A burette with an inserted Cu rod to connect the high-voltage supply was filled with the electrostatic spinning solution. An aluminum foil was served as the counter electrode. The distance between the burette tip and receiver was fixed at 14 cm. the high-voltage supply was fixed at 14 kV. The spinning rate was controlled at about 0.7 mL/h by adjusting the angle of inclination of the burette. The electrospinning was performed at 25°C. The spinning time was 4 h. The uniform edge was selected as the sample for electron microscopy tests. The electrospinning apparatus used here was almost the same as that has been used in the reported work.[19a]

Preparation of test strip

The filter paper was sticked on the aluminum foil. The electrostatic spinning process was the same as that in "Preparation of electrostatic spinning solution and film" except the spinning time was 20 h. The nano wires were adhered to the filter paper and formed a thin film. The thin film and the filter paper were cut into strips with a paper knife for tests.

Conclusions

A mononuclear zinc complex was synthesized as a highly selective naked-eye-based chemosensor for PPi in aqueous solution. Because the complex formation inhibits the keto-enol transformation process, the color of ethanol solution of the complex is red even in the presence of 10 wt% water. The introduction of PPi made PPi coordinate zinc ion and the oxygen of the phenolic hydroxyl group was released, and thus compound **L** was reformed, which brought about the occurrence of the keto–enol transformation in the presence of trace water and made the color of the sensor change from red to colorless. Moreover, via electrospinning, the complex nanofiber was successfully prepared and the color of the nanofiber changed from red to colorless after they were immersed into aqueous solution of pyrophosphate and the nanofibers had high selectivity toward PPi.

Acknowledgments

Notes and references

College of Chemistry and Molecular Engineering, Zhengzhou University, Zhengzhou 450001, China. E-mail: lizx@zzu.edu.cn; yumm@zzu.edu.cn; weiliuhe@zzu.edu.cn. Tel.: +86 371 67781205; fax: +86 371 67781205
† Electronic Supplementary Information (ESI) available Crystallographic data for compounds **1** and **L**. CCDC-960149 and CCDC-1019895. For crystallographic data in CIF see DOI: 10.1039/b000000x/

1   C. P. Mathews and K. E. Hold, Biochemistry, Benjamin/Cummings Publishing Co., Redwood City, CA, 1990.
2   M. Ronaghi, S. Karamohamed, B. Pettersson, M. Uhlen and P. Nyren, *Anal. Biochem.*, 1996, **242**, 84–89.
3   S. Q. Xu, M. He, H. P. Yu, X. K. Cai, X. L. Tan, B. Lu and B. H. Shu, *Anal. Biochem.*, 2001, **299**, 188–193.
4   (a) Y. Li, X. Dong, C. Zhong, Z. Liu and J. Qin, *Sens. Actuator B*, 2013, **183**, 124–128; (b) R.-M. Kong, T. Fu, N.-N. Sun, F.-L. Qu, S.-F. Zhang and X.-B. Zhang, *Biosens. Bioelectron.*, 2013, **50**, 351–355; (c) S. Liu, S. Pang, W. Na and X. Su, *Biosens. Bioelectron.*, 2014, **55**, 249–254; (d) B. K. Datta, S. Mukherjee, C. Kar, A. Ramesh and G. Das, *Anal. Chem.*, 2013, **85**, 8369–8375; (e) X. Zhu, J. Yang and K. S. Schanze, *Photochem. Photobiol. Sci.*, 2014, **13**, 293–300; (f) J. Wang, W. Chen, X. Liu, C. Wesdemiotis and Y. Pang, *J. Mater. Chem. B*, 2014, **2**, 3349–3354; (g) P. Das, N. B. Chandar, S. Chourey, H. Agarwalla, B. Ganguly and A. Das, *Inorg. Chem.*, 2013, **52**, 11034–11041; (h) Y. Mikata, A. Ugai, R. Ohnishi and H. Konno, *Inorg. Chem.*, 2013, **52**, 10223–10225; (i) S. Anbu, R. Ravishankaran, M. F. C. Guedes da Silva, A. A. Karande and A. J. L. Pombeiro, *Inorg. Chem.*, 2014, **53**, 6655–6664; (j) A. K. Mahapatra, S. K. Manna, C. Das Mukhopadhyay and D. Mandal, *Sens. Actuator B*, 2014, **200**, 123–131.
5   (a) W. Yu, J. Qiang, J. Yin, S. Kambam, F. Wang, Y. Wang and X. Chen, *Org. Lett.*, 2014, **16**, 2220–2223; (b) X. Liu, N. Huy Tien, Z. Ge, S. J. Butler and K. A. Jolliffe, *Chem. Sci.*, 2013, **4**, 1680–1686; (c) S. Goswami, S. Paul and A. Manna, *RSC Adv.*, 2013, **3**, 10639–10643.
6   M. Maue and T. Schrader, *Angew. Chem., Int. Ed.*, 2005, **44**, 2265–2270.
7   D. R. Weinberg, C. J. Gagliardi, J. F. Hull, C. F. Murphy, C. A. Kent, B. C. Westlake, A. Paul, D. H. Ess, D. G. McCafferty and T. J. Meyer, *Chem. Rev.*, 2012, **112**, 4016–4093.
8   (a) J. Waluk, *Acc. Chem. Res.*, 2003, **36**, 832–838; (b) L. M. Tolbert and K. M. Solntsev, *Acc. Chem. Res.*, 2002, **35**, 19–27; (c) M. S. Baranov, K. A. Lukyanov, A. O. Borissova, J. Shamir, D. Kosenkov, L. V. Slipchenko, L. M. Tolbert, I. V. Yampolsky and K. M. Solntsev, *J. Am. Chem. Soc.*, 2012, **134**, 6025–6032.
9   Y. Yang, Q. Zhao, W. Feng and F. Li, *Chem. Rev.*, 2013, **113**, 192–270.
10 (a) X. Liu, J. Li, C. Hu, Q. Zhou, W. Zhang, M. Hu, J. Zhou and J. Wang, *Angew. Chem., Int. Ed.*, 2013, **52**, 4805–4809; (b) Z. Xu, K.-H. Baek, H. N. Kim, J. Cui, X. Qian, D. R. Spring, I. Shin and J. Yoon, *J. Am. Chem. Soc.*, 2010, **132**, 601–610; (c) M. A. Palacios, Z. Wang, V. A. Montes, G. V. Zyryanov and P. Anzenbacher, Jr., *J. Am. Chem. Soc.*, 2008, **130**, 10307–10314.
11 (a) B. K. Datta, S. Mukherjee, C. Kar, A. Ramesh and G. Das, *Anal. Chem.*, 2013, **85**, 8369–8375; (b) Y. Mikata, A. Ugai, R. Ohnishi and H. Konno, *Inorg. Chem.*, 2013, **52**, 10223–10225.
12 F. A. S. Chipem and G. Krishnamoorthy, *J Phys. Chem. A*, 2009, **113**, 12063–12070.
13 (a) A. Brenlla, M. Veiga, J. L. Perez Lustres, M. C. Rios Rodriguez, F. Rodriguez-Prieto and M. Mosquera, *J Phys. Chem. B*, 2013, **117**, 884–896; (b) S.-Y. Park, Y. Kim, J. Y. Lee and D.-J. Jang, *J Phys. Chem. B*, 2012, **116**, 10915–10921.
14 A. Brenlla, F. Rodriguez-Prieto, M. Mosquera, M. A. Rios and M. C. Rios Rodriguez, *J. Phys. Chem. A*, 2009, **113**, 56–67.
15 Z. Li, X. Liu, W. Zhao, S. Wang, W. Zhou, L. Wei and M. Yu, *Anal. Chem.*, 2014, **86**, 2521–2525..
16 J.-H. Syu, Y.-K. Cheng, W.-Y. Hong, H.-P. Wang, Y.-C. Lin, H.-F. Meng, H.-W. Zan, S.-F. Horng, G.-F. Chang, C.-H. Hung, Y.-C. Chiu, W.-C. Chen, M.-J. Tsai and H. Cheng, *Adv. Funct. Mater.*, 2013, **23**, 1566–1574.
17 Y. Wang, B. Li, Y. Lin, L. Zhang, Q. Zuo, L. Shi and Z. Su, *Chem. Commun.*, 2009, 5868–5870.
18 W. Wang, Q. Yang, L. Sun, H. Wang, C. Zhang, X. Fei, M. Sun, Y. Li, *J. Hazard. Mater.*, 2011, **194**, 185–192.
19 (a) Y. Yang, H. Wang, K. Su, Y. Long, Z. Peng, N. Li and F. Liu, *J. Mater. Chem.*, 2011, 11895–11900; (b) C. Wolf, M. Tscherner and S. Köstler, *Sens. Actuators, B*, 2015, **209**, 1064–1069; (c) J. Song, W. Zhang, K. Miao, H. Zeng, S. Cheng, and L. J. Fan, *ACS Appl. Mater. Inter.*, 2013, **5**, 4011–4016; (d) W. Wang, Y. Li, M. Sun, C. Zhou, Y. Zhang, Y. Li and Q. Yang, *Chem. Commun.*, 2012, **48**, 6040–6042.
20 S. Bhowmik, B. N. Ghosh, V. Marjomaki and K. Rissanen, *J. Am. Chem. Soc.*, 2014, **136**, 5543–5546.
21 Q.-C. Xu, X.-F. Wang, G.-W. Xing, Y. Zhang, *RSC Adv.*, 2013, **3**, 15834–15841.
22 Characterization of the isolated product from the reaction of **ZnLCl₂** with PPi: HRMS (EI) m/z: calcd for $C_{20}H_{18}N_2O_4$ [M + Na]$^+$, 373.1159; found, 373.1165. ^{1}H NMR (400 MHz, CDCl$_3$, TMS): δ_H 9.14(s, 1H), 8.39 (d, 1H), 8.25 (d, 1H), 7.50 (m, 3H), 7.28 (m, 1H), 7.06 (m, 2H), 6.97 (m, 2H), 5.04 (s, 2H), 4.33 (q, 2H), and 1.32 (t, 3H). ^{13}C NMR (100 MHz, CDCl$_3$): δ_C 168.63, 157.51, 153.91, 153.60, 152.92, 139.97, 136.67, 134.39, 130.26, 127.91, 120.97, 120.38, 118.94, 116.40, 115.39, 110.32, 66.40, 61.55, and 14.21.
23 The relevant crystal data and structural parameters are: formula: $C_{20}H_{18}N_2O_4$. M = 350.36, monoclinic. Unit cell parameters: a = 17.9227(13) Å, b = 5.0106(3) Å, c = 20.9309(16) Å. α = 90.00°, β = 114.168(9)°, γ = 90.00°, V = 1714.9(2) Å^3, T = 273(2) K, space group P 21/n, Z = 4, 5964 reflections collected, 3002 independent reflections [R(int) = 0.0303]. Final R indices [I > 2σ(I)] R1 = 0.0552 and wR2 = 0.1498. R indices (all data) R1 = 0.1041 and wR2 = 0.1305.
24 SMART and SAINT. Area Detector Control and Integration Software; Siemens Analytical X-Ray Systems, Inc.: Madison, WI(USA) 1996.
25 G.M. Sheldrick, SADABS 2.05, University of Göttingen, Germany.
26 (a) G. M. Sheldrick, *Acta Crystallogr. Sect. A (Foundations of Crystallography)*, 1990, **A46**, 467–473; (b) G. M. Sheldrick, SHELXS-97, Program for solution of crystal structures, University of Göttingen, Germany, 1997.
27 G.M. Sheldrick, *Acta Crystallogr. Sect. A*, 2008, **64**, 112–122.

Naked-eye-based selective detection of pyrophosphate with Zn^{2+} complex in aqueous solution and electrospun nanofibers

Zhanxian Li,* Wenying Zhang, Xingjiang Liu, Chunxia Liu, Mingming Yu,* Liuhe Wei*
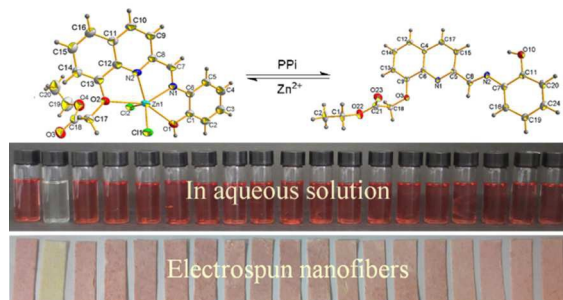
5

Based on keto-enol transformation process, a zinc complex as a naked-eye-based chemosensor for pyrophosphate in aqueous solution and electrospun nanofibers has been developed.